Distinct hepatic lipid profile of hypertriglyceridemic mice determined by easy ambient sonic-spray ionization mass spectrometry

Luciane C. Alberici, Helena C. F. Oliveira, Rodrigo R. Catharino, Anibal E. Vercesi, Marcos N. Eberlin & Rosana M. Alberici

Analytical and Bioanalytical Chemistry

ISSN 1618-2642

Anal Bioanal Chem
DOI 10.1007/
s00216-011-5208-8

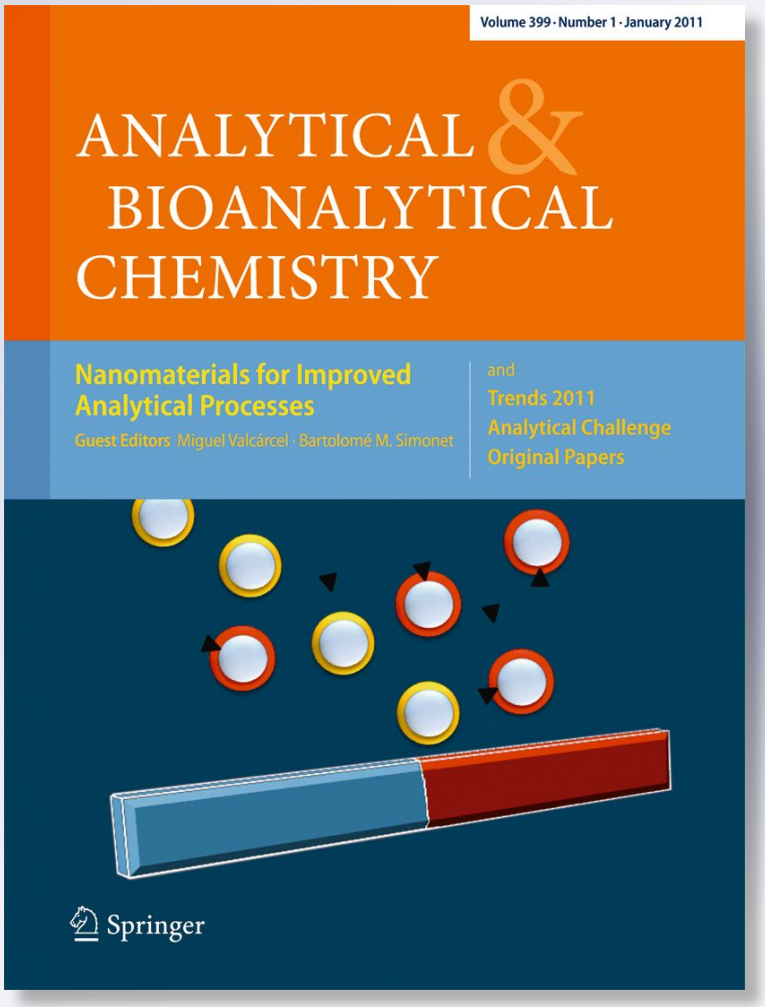

Springer

Anal Bioanal Chem
DOI 10.1007/s00216-011-5208-8

ORIGINAL PAPER

Distinct hepatic lipid profile of hypertriglyceridemic mice determined by easy ambient sonic-spray ionization mass spectrometry

Luciane C. Alberici · Helena C. F. Oliveira · Rodrigo R. Catharino · Anibal E. Vercesi · Marcos N. Eberlin · Rosana M. Alberici

Received: 12 March 2011 / Revised: 13 June 2011 / Accepted: 24 June 2011

Abstract Easy ambient sonic-spray ionization mass spectrometry (EASI-MS) was used to interrogate the hepatic lipid profiles of hypertriglyceridemic and control normotriglyceridemic mice. The analyses of ex vivo complex lipid mixtures were made directly with EASI-MS without accompanying separation steps. Intense ions for phosphatidylcholines and triacylglycerols were observed in the positive ion mode whereas the spectra in the negative ion mode provided profiles of phosphatidylethanolamines and phosphatidylinositol. EASI-MS was coupled to high-performance thin-layer chromatography for analysis of free fatty acids. Fourier transform–ion cyclotron resonance–mass spectrometry was also employed to confirm the identity of the detected lipids. We demonstrated higher incorporation of oleic acid in phosphatidylcholine and triacylglycerol composition, higher relative abundance of arachidonic acid containing phosphatidylinositol, and overall distinct free fatty acid profile in the livers of genetic hypertriglyceridemic mice. We propose that these alterations in liver lipid composition are related to the higher tissue and body metabolic rates described in these hypertriglyceridemic mice.

Keywords Hypertriglyceridemia · Mice liver · Ambient ionization · Mass spectrometry · Lipids

L. C. Alberici (✉)
Department of Physics and Chemistry, Faculty of Pharmaceutical Sciences, University of São Paulo, USP,
Ribeirão Preto, São Paulo 14040-903, Brazil
e-mail: alberici@fcfrp.usp.br

H. C. F. Oliveira
Physiology and Biophysics Division, Biology Institute,
University of Campinas, UNICAMP,
Campinas, São Paulo 13083-970, Brazil

R. R. Catharino · A. E. Vercesi
Department of Clinical Pathology, Faculty of Medical Sciences,
University of Campinas, UNICAMP,
Campinas 13083-887, SP, Brazil

M. N. Eberlin · R. M. Alberici
ThoMSon Mass Spectrometry Laboratory, Institute of Chemistry,
University of Campinas, UNICAMP,
Campinas 13083-970, SP, Brazil
e-mail: rmalberici@iqm.unicamp.br

Introduction

Hypertriglyceridemia is an independent risk factor for atherosclerotic coronary heart disease, stroke, and nonalcoholic fatty liver disease [1–3]. Genetically modified mice overexpressing human apolipoprotein (Apo) C-III (hypertriglyceridemic) have elevated triacylglycerols (TAG) levels due to the presence of enlarged TAG-rich lipoproteins in plasma [4–6]. Apo C-III in excess delays the clearance of TAG-rich lipoproteins, and their prolonged residence time in plasma continuously provides more free fatty acids (FFA) to the peripheral tissues. High plasma FFA levels lead to increased uptake of FFA into non-adipose tissues such as liver and may contribute to intracellular lipid accumulation. In a previous work, using an enzymatic–colorimetric assay, we showed that hypertriglyceridemic mice liver presented a fivefold elevation in the content of total glycerolipids as compared with control livers [7].

We have also demonstrated that liver mitochondria isolated from hypertriglyceridemic mice presented higher resting O_2 consumption rates [8]. Intracellular fatty acid content is probably implicated in this process, since respiratory rates were totally corrected by treatment of hypertriglyceridemic mice with fibrates, which activate

Published online: 06 July 2011

fatty acid β-oxidation and decrease the content of intracellular lipids. The higher resting respiratory rates occur due to mild mitochondrial uncoupling promoted by the stimulated activity of the ATP-sensitive potassium channel. Accordingly, these mice presented increased whole-liver oxygen consumption, increased whole body metabolic rate, and higher food intake, without enhanced weight gain [9]. Now, we focus our attention on the liver lipid profile that might be involved in increased metabolism of hypertriglyceridemic liver. We hypothesize that not only the total amount of FFA but also the differential content of FFA species may be responsible for the metabolic effects described in the liver of these mice.

Mass spectrometry (MS) has been established as a powerful analytical tool with increasing use in the analysis of complex lipid mixtures in lipidomic studies [10–13]. Electrospray ionization (ESI) [14], atmospheric pressure chemical ionization [15], and matrix-assisted laser desorption/ionization [16] are well-established ionization techniques that allow lipids to be analyzed by MS with high sensitivity and no or little fragmentation. However, the ability of these techniques to detect the individual lipid classes differs significantly. Due to the presence of the quaternary ammonium group in its head group, phosphatidylcholine and sphingomyelin are strongly cationic and ionize well in the positive ion mode. This easy ionization may cause the suppression of less polar lipids. Complex lipid mixtures require therefore previous chromatographic separation into the individual lipids or lipid classes [17]. High-performance thin-layer chromatography (HPTLC) makes use of silica gel of a very uniform and small particle size, permitting excellent separations with comparatively short elution times [18]. Secure spot characterization in HPTLC requires, however, coupling with other techniques [19]. HPTLC provides a proper surface in which direct on-spot desorption and ionization of analytes can be performed [20]. Several MS techniques have been applied to characterize HPTLC spots, and it has been facilitated by employing ambient MS ionization methods [21–24]. Easy ambient sonic-spray ionization mass spectrometry (EASI-MS) [25, 26] is an ambient ionization technique [21] which allows the direct and fast MS analysis of samples in the open atmosphere with little or no sample preparation. In EASI, the sonic spray creates droplets of solvent (e.g., methanol) which end up being charged (both positively and negatively) due to statistical unbalanced distribution of cations and anions in these very minute droplets with limited charge-carrying capability. The dense stream of the sonic (bipolar) charged droplets promotes analyte pick up from the surface, concomitant ionization as either cations or anions, and then transfer of the analyte ions to the gas phase for further mass analysis. Ionization by EASI is soft, causing no or minimum fragmentation [21]. We have recently combined TLC with EASI-MS for on-spot detection and characterization of pharmaceutical drugs and vegetable oils [27], and HPTLC with EASI-MS for the quality control of biodiesel and biodiesel–petrodiesel blends [28].

Herein, we investigate the application of direct EASI-MS analysis to disclose the phospholipids and TAG profiles that might be involved in increased metabolism of livers from hypertriglyceridemic mice. EASI-MS was also coupled to HPTLC for analysis of FFA due the ionic suppression caused by phospholipids (mainly phosphatidylethanolamine) in the negative mode.

Experimental

Chemicals and reagents

HPLC-grade methanol, diethyl ether, *n*-hexane, and chloroform were purchased from Merck SA and used without further purification. FFA, TAG, and phospholipids used as standards were from Sigma (Deisenhofen, Germany).

Animals

Human apolipoprotein C-III transgenic (line 3707) [29] crossbred with wild-type C57Bl6 mice have been maintained for the last 14 years at the animal facilities of the Department of Physiology and Biophysics at the State University of Campinas (Campinas, Brazil). The experiments were approved by the university's ethics committee and are in accordance with the Guidelines for Handling and Training of Laboratory Animals published by the University's Federation for Animal Welfare. Mice had access to standard laboratory rodent chow (CR1; Nuvital, Colombo, Paraná, Brazil) and water ad libitum and were housed at 22±2 °C on a 12-h light–dark cycle. Six female heterozygous apolipoprotein C-III transgenic (hypertriglyceridemic) and six non-transgenic (normotriglyceridemic) littermates, aged 4 months, were used in this study. Total TAG (Roche Diagnostic GmbH, Mannheim, Germany) levels were determined by enzymatic–colorimetric methods according to the manufacturers' instructions. Hypertriglyceridemic mice presented fasting plasma TAG levels >300 mg/dL and normotriglyceridemic mice levels <100 mg/dL.

Lipid extraction

Animals were killed by cervical dislocation and approximately 300 mg of each liver were rapidly homogenized in 1 ml of cold chloroform (4 °C) separately. The liver lipids were extracted adding 2 ml methanol and 0.8 ml water, according to Bligh and Dyer [30]. The lower chloroform

layer was dried under a stream of nitrogen and dissolved in 0.05 ml chloroform to immediate analyzes. Each lipid extract represents a single animal.

High-performance thin-layer chromatography

Only for FFA analysis by EASI-MS, lipids were separated on HPTLC plates (silica gel 60 plates without fluorescent indicator, Merck, Darmstadt, Germany). Lipid extracts (2 μL) were run in a solvent mixture composed of hexane/diethyl ether/acetic acid (80:20:1.5 *v/v*) in an automatic developing chamber (ADC 2, CAMAG, Muttenz, Switzerland) previously saturated with the same solvent system (20 mL) for 20 min (25±2 °C, relative humidity 75%). The plates were then dried. Lipid spots were identified by UV light (λ=254 nm) and circled using a pencil. Images of chromatograms were taken with a photographing system. The identity of the lipids in each spot was established by comparison with the R_f values measured for authentic standards. After HPTLC separation, EASI-MS was performed by spraying along the whole spot of FFA to promote their desorption/ionization and MS characterization [27]. The whole spot was scanned to get a representative spectrum.

Easy ambient sonic-spray ionization mass spectrometry

Liver extracts were analyzed in duplicate in both the positive and negative ion modes, using a single-quadrupole mass spectrometer (Shimadzu) equipped with a homemade EASI source [25, 26]. The main experimental parameters were as follows: The flow rate of methanol was set at 20 μL min^{-1}, N_2 nebulizing gas in flow rate of 3 L min^{-1}, and paper (or capillary-HPTLC plate)-entrance angle of ~30°. When using samples without previous separation, a tiny droplet (2 μL) of the liver extracts was dropped directly onto the paper surface (brown Kraft paper) and let dry. Mass spectra were accumulated over 60 s and scanned along the *m/z* 50 to 1,000 range. When operating in the negative ion mode, the methanol solvent was doped with 0.1% of the ammonium hydroxide. Standard TAG and phospholipids were dissolved in chloroform, at a final concentration of 1 mmol L^{-1}, and efficiency of ionization for TAG and phospholipids was calculated by the ratio of intensities of TAG/more abundant phospholipids. Results obtained show that CV is around 10% (data not show).

Fourier transform–ion cyclotron resonance–mass spectrometry

Liver extracts diluted in methanol (100 μL) were loaded into a 96-well plate, and an automated chip-based nano-ESI system (Triversa NanoMate 100; Advion BioSciences, Ithaca, NY, USA) was used for injecting the solution at a rate of 0.2 μL/min in the Fourier transform–ion cyclotron resonance–mass spectrometry (FT-ICR-MS) equipment. Mass spectra were collected in both the positive and negative ion modes in a LTQ FT Ultra mass spectrometer (ThermoScientific, Bremen, Germany). NanoMate general conditions were: gas pressure, 0.3 psi and capillary voltage, 1.55 kV. Mass spectra were accumulated over 5 min, scanned over the 200–1,000 *m/z* range, centered, and aligned using the Xcalibur 2.0 software (ThermoScientific, Bremen, Germany). The high mass accuracy obtained using FT-ICR-MS (typically 0.1 ppm) allows unequivocal attribution of TAG molecular composition.

Data analysis

Lipid analyses from each preparation were made in duplicate, and averages were calculated. Data shown as spectrum are representative of each group, and other data are ratio averages ±SEM. Statistical analysis was performed using Mann–Whitney non-parametric test conducted using Origin 7.0 software (Origin Lab Corp., Northampton, MA). $P<0.05$ was considered significant.

Results

Liver lipid extracts from normotriglyceridemic and hypertriglyceridemic mice were directly analyzed by EASI-MS. Figure 1 shows representative EASI mass spectra in the positive ion mode of the lipid mixtures from normotriglyceridemic (Fig. 1a) and hypertriglyceridemic (Fig. 1b) mice. The lipid profiles appear within the *m/z* 750 to 950 range and show both phospholipid and TAG ions. The phospholipid ions corresponding to those detected in other lipidomic MS studies performed using electrospray ionization mass spectrometry (ESI-MS) [31] or desorption ESI-MS [32–34]. The phosphatidylcholines can be detected as $[M+H]^+$, $[M+Na]^+$, and $[M+K]^+$ adducts as a result of endogenous sodium and potassium salts in these tissues. EASI favors the ionization of the sodium species $[M+Na]^+$. The abundant phosphatidylcholine ions are consistent with the knowledge that these species constitute the majority of biological membranes [35]. None of the major ions are due to sphingomyelin since all have even *m/z* values (sphingomyelin contain two nitrogen and display, therefore, even masses). Table 1 summarizes the major ions detected in the EASI(+) spectra.

In the positive ion mode, the ion of *m/z* 780, the most intense ion phospholipid of the spectra, was used as reference to compare the profiles from hypertriglyceridemic and normotriglyceridemic liver obtained by EASI-MS. The spectra clearly show an increased intensity of

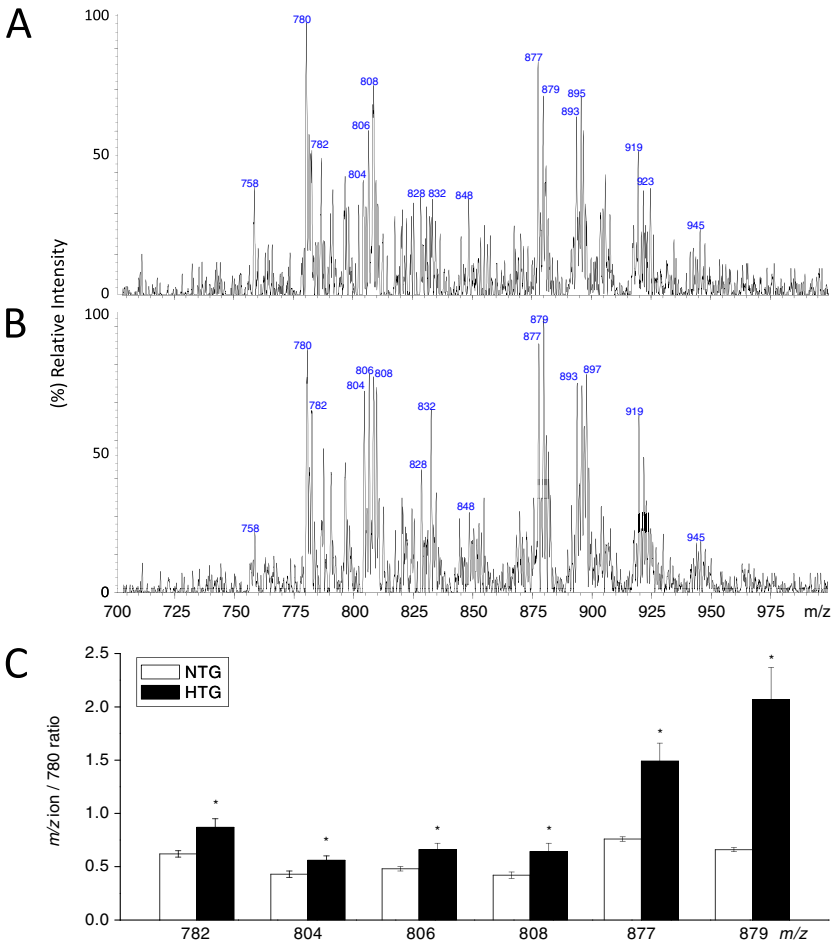

Fig. 1 Representative EASI (positive ion mode) mass spectra of six different liver extracts from **A** normotriglyceridemic and **B** hypertriglyceridemic mice. **C** Averages±SEM of ion intensities relative to *m/z* 780

[phosphatidylcholine+Na]$^+$ ions of *m/z* 782, 804, 806, 808, 828, and 832 relative to phosphatidylcholine *m/z* 780 for the hypertriglyceridemic liver (Fig. 1b) as compared with normotriglyceridemic (Fig. 1a). Some of the phosphatidylcholine ions detected, such as *m/z* 782 and 806 includes two isobaric phosphatidylcholine species, [PC 34:1+Na]$^+$ or [PC 36:4+H]$^+$, which can only be differentiated with tandem mass spectrometry [36] or with a

Table 1 Assignment of the lipids forming major ions in the positive ion mode EASI mass spectra of the normotriglyceridemic and hypertriglyceridemic mice liver extracts

MM	[M+H]$^+$	[M+Na]$^+$	[M+K]$^+$	Assignment[a]	Elemental composition[b]
757	758	780	796	PC 34:2	$C_{42}H_{80}NO_8P$
759	760	782	798	PC 34:1	$C_{42}H_{82}NO_8P$
781	782	804	820	PC 36:4	$C_{44}H_{80}NO_8P$
783	784	806	822	PC 36:3	$C_{44}H_{82}NO_8P$
785	786	808	824	PC 36:2	$C_{44}H_{84}NO_8P$
805	806	828	844	PC 38:6	$C_{46}H_{80}NO_8P$
809	810	832	848	PC 38:4	$C_{46}H_{84}NO_8P$
852	–	875	891	TAG 52:5	$C_{55}H_{96}O_6$
854	–	877	893	TAG 52:4	$C_{55}H_{98}O_6$
856	–	879	895	TAG 52:3	$C_{55}H_{100}O_6$
858	–	881	897	TAG 52:2	$C_{55}H_{102}O_6$
860	–	883	899	TAG 52:1	$C_{55}H_{104}O_6$
880	–	903	919	TAG 54:5	$C_{57}H_{100}O_6$
882	–	905	921	TAG 54:4	$C_{57}H_{102}O_6$
884	–	907	923	TAG 54:3	$C_{57}H_{104}O_6$

PC phosphatidylcholine, *TAG* triacylglycerol

[a] Carbon number followed by the number of unsaturated bonds

[b] Identified by FT-ICR-MS

higher-resolution instrument. High-resolution mass spectrometry is one of the most valuable tools for lipid analysis because it can provide exact molecular weights and unique spectra to aid in identification of unknown compounds. In this work, chemical assignments (Table 1) were confirmed by FT-ICR-MS. Since the palmitic (16:0), stearic (18:0), oleic (18:1), and linoleic (18:2) acids are the most predominantly fatty acid in hepatic phosphatidylcholine [37], the most abundant phosphatidylcholine ion of *m/z* 780 (34:2) probably is composed by palmitic/linoleic acids whereas palmitic/oleic acids compose the phosphatidylcholine ions of *m/z* 782 (34:1). The decreased *m/z* 780/782 ratio in hypertriglyceridemic livers (Fig. 1c) means therefore that the hypertriglyceridemic liver presents higher proportion of oleic acid in its 34 carbons phosphatidylcholine compared with the normotriglyceridemic liver. A higher content of the phosphatidylcholine ions of *m/z* 804, 806, and 808 (36:4, 36:3, and 36:2) relative to phosphatidylcholine *m/z* 780 in the hypertriglyceridemic liver (Fig. 1c) was also observed. Among them, the ions of *m/z* 806 and 808 ions are probably composed by linoleic/oleic and oleic/oleic acids, respectively, again indicating a higher incorporation of oleic acid in the phosphatidylcholine in the hypertriglyceridemic liver.

In addition to phosphatidylcholine ions, EASI(+)-MS was also able to detect TAG ions contained in the livers from normotriglyceridemic (Fig. 1a) and hypertriglyceridemic (Fig. 1b) mice in the *m/z* range 850 to 950. TAG were detected mostly as the $[TAG+Na]^+$ and $[TAG+K]^+$ ions with undetectable protonated molecules [16, 38, 39]. The identification of the main TAG detected as such ions (Table 1) shows that the ions of *m/z* 877 (52:4) and *m/z* 879 (52:3) significantly contribute to the TAG composition profiles of both mice livers. The spectra clearly show that the TAG ion of *m/z* 879 is significantly more intense (the base ion) in the hypertriglyceridemic spectrum in comparison to the normotriglyceridemic spectrum. The comparison of the intensities of the TAG ions of *m/z* 877 (52:4) and *m/z* 879 (52:3) indicates that the TAG ion of *m/z* 877 is predominant in liver from normotriglyceridemic whereas *m/z* 879 is predominant in liver from hypertriglyceridemic mice. Moreover, hypertriglyceridemic liver also presented TAG ions of *m/z* 877, 897, and 919 (relative to the PC ion of *m/z* 780) of increased intensity compared with normotriglyceridemic liver (see also the *m/z* 780/877 and 780/879 ratios in Fig. 1c). These results indicate higher levels of TAG in hypertriglyceridemic liver. Since the palmitic (16:0), oleic (18:1), and linoleic (18:2) acids are the most predominantly fatty acid in hepatic TAG [40], our results indicate that the predominant TAG ion of *m/z* 877 (52:4) in normotriglyceridemic livers probably is composed by palmitic/linoleic/linoleic acids whereas in the hypertriglyceridemic livers the predominant TAG ion of *m/z* 879 (52:3) is probably composed of palmitic/oleic/linoleic acids. It means a change from one linoleic to oleic acid in the TAG from normotriglyceridemic compared with hypertriglyceridemic liver.

Figure 2 shows representative spectra EASI mass in the negative ion mode with profiles of liver lipids from normotriglyceridemic (Fig. 2a) and hypertriglyceridemic (Fig. 2b) mice. Phosphatidylcholine is generally undetectable in the negative ion mode due to permanent positive charge located on the quaternary amine in the head groups of such lipids. But phosphatidylethanolamines, phosphati-

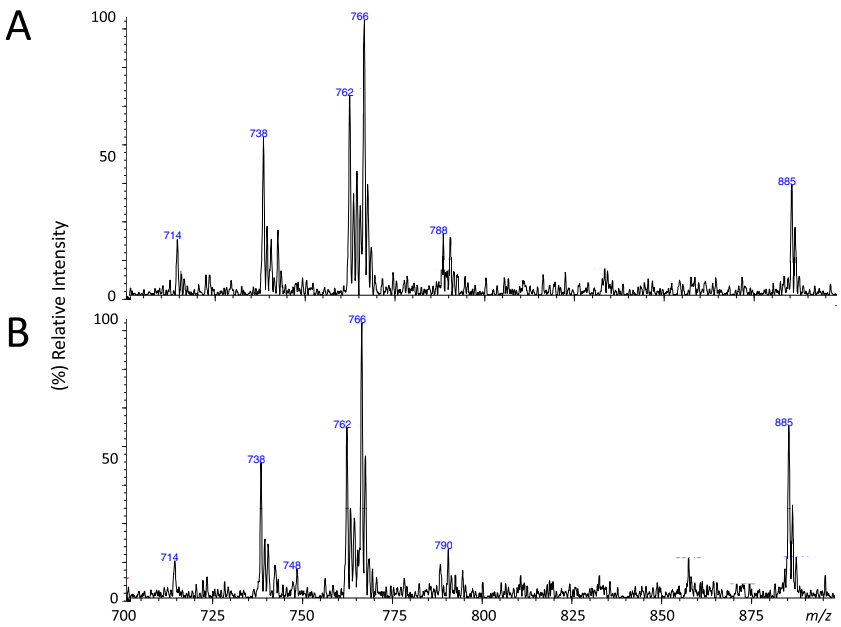

Fig. 2 Representative EASI (negative ion mode) mass spectra of six different liver extracts from **A** normotriglyceridemic and **B** hypertriglyceridemic mice

dylserines, phosphatidylinositols, and sulfatides ionize much more efficiently in the negative mode due to ionization of phosphate group as $R\text{-}PO_3^-$. The EASI(−) mass spectra show that phosphatidylethanolamine dominate and are detected exclusively as $[M-H]^-$ ions. Table 2 shows the identity of the major ions detected in the EASI (−)-MS for these lipid mixtures. The intensity of the major ions phosphatidylethanolamine of *m/z* 738, 762, 766, 788, and 790 were very similar for both normotriglyceridemic and hypertriglyceridemic mice. The phosphatidylinositol ion of *m/z* 885 (38:4) was more intense in the livers from hypertriglyceridemic mice (*m/z* 766/885 ratio, 2.52±0.2 vs. 1.56±0.3 for hypertriglyceridemic and normotriglyceridemic, respectively) and was identified by FT-ICR-MS with side-chains 18:0 and 20:4, in which 20:4 is the arachidonate.

In the EASI(+)-MS (Fig. 1), no DAG species were detected in the *m/z* range 600 to 700 (not shown). Moreover, very low intensities of FFA in the *m/z* 150–400 range (not shown) were detected in the EASI(−)-MS spectra (Fig. 2). These show preferential ionization of phosphatidylethanolamine lipids. To ascertain the FFA composition in mice livers, the lipid extracts were separated by HPTLC [18], which is a relatively simple and easy to perform chromatographic separation able to resolve each of the main simple lipids from a tissue such as cholesterol esters, TAG, DAG, FFA, and cholesterol. During HPTLC, lipids such as phospholipids will remain at the origin when using hexane and diethyl ether as mobile phase. Control experiments were conducted with standards, and their spots were determinate by UV exposure showing completely perfect separation of TAG from DAG, phospholipids, and FFA (data not shown). Figure 3a, b shows the HPTLC of the liver organic extracts from normotriglyceridemic mice and hypertriglyceridemic mice. Note that sufficient resolution leads to good separation of the three major lipids components, in high to low R_f order: FFA, TAG, and phospholipids. Phospholipids are considerably more polar and therefore display a much lower R_f. The detection of greater spot for the TAG from hypertriglyceridemic liver confirms the results obtained to EASI-MS (Fig. 1).

Figure 3a, b shows EASI(−)-MS of the highest R_f spot (FFA) of normotriglyceridemic and hypertriglyceridemic livers. As expected, hypertriglyceridemic spectrum (Fig. 3b) displays a much more diverse profile of FFA compared to normotriglyceridemic (Fig. 3a). The main ions detected were the $[FFA-H]^-$ ions of *m/z* 253, 255, 281, and 283, which correspond to palmitoleic, palmitic, oleic, and stearic acids (Table 2), respectively, with predominant signal from palmitic acid. Using the most intense FFA ion of *m/z* 255 as reference, a clear increase in the intensity of the FFA ions of *m/z* 253, 269 (margaric acid), 281, 283, and 303 (arachidonic acid) is seem in the hypertriglyceridemic spectrum as compared with normotriglyceridemic (see also Fig. 3c). These results demonstrate characteristic FFA profiles in the hypertriglyceridemic liver. The ionization of the same spot by EASI(+) detected no DAG ions, revealing that DAG was in fact undetectable. The second and third spots, corresponding to TAG and phosphatidylcholine, respectively, showed very similar lipid profiles (data not shown) as those shown in Fig. 1.

Table 2 Assignment of the lipids forming major ions in the negative ion mode EASI mass spectra of the normotriglyceridemic and hypertriglyceridemic mice liver extracts

MM	$[M-H]^-$	Assignment[a]	Elemental composition[b]
254	253	FA 16:1	$C_{16}H_{30}O_2$
256	255	FA 16:0	$C_{16}H_{32}O_2$
270	269	FA 17:0	$C_{17}H_{34}O_2$
282	281	FA 18:1	$C_{18}H_{34}O_2$
284	283	FA 18:0	$C_{18}H_{36}O_2$
304	303	FA 20:4	$C_{20}H_{32}O_2$
741	738	PE 36:4	$C_{41}H_{74}NO_8P$
743	742	PE 36:2	$C_{41}H_{78}NO_8P$
765	762	PE 38:6	$C_{43}H_{74}NO_8P$
767	766	PE 38:4	$C_{43}H_{78}NO_8P$
789	788	PE 40:7	$C_{45}H_{76}NO_8P$
791	790	PE 40:6	$C_{45}H_{78}NO_8P$
886	885	PI 38:4	$C_{47}H_{82}O_{13}P$

FA fatty acid, *PE* phosphatidylethanolamine, *PI* phosphatidylinositol

[a] Carbon number followed by the number of unsaturated bonds

[b] Identified by FT-ICR-MS

Discussion

High plasma FFA and TAG levels lead to increased uptake of FFA into non-adipose tissues and contribute to intracellular lipid accumulation. In our previous report, we have shown higher glycerolipids accumulation in the liver of hypertriglyceridemic mice determined by an enzymatic–colorimetric (indirect) assay [7]. Here, EASI-MS and HPTLC-EASI-MS analyses reinforce this result and also revealed distinct TAG, phospholipid, and FFA profiles in hypertriglyceridemic livers.

Higher TAG content was demonstrated by decreased PC/TAG ratio in the hypertriglyceridemic liver spectrum. In addition, a higher insertion of oleic acid (18:1) relative to linoleic acid (18:2) was found to be predominant in TAG (52C) from hypertriglyceridemic livers. Oleic acid was also abundant in phosphatidylcholine composition of the hypertriglyceridemic liver. In eukaryotic membranes, phosphatidylcholine often constitutes almost 50% of the

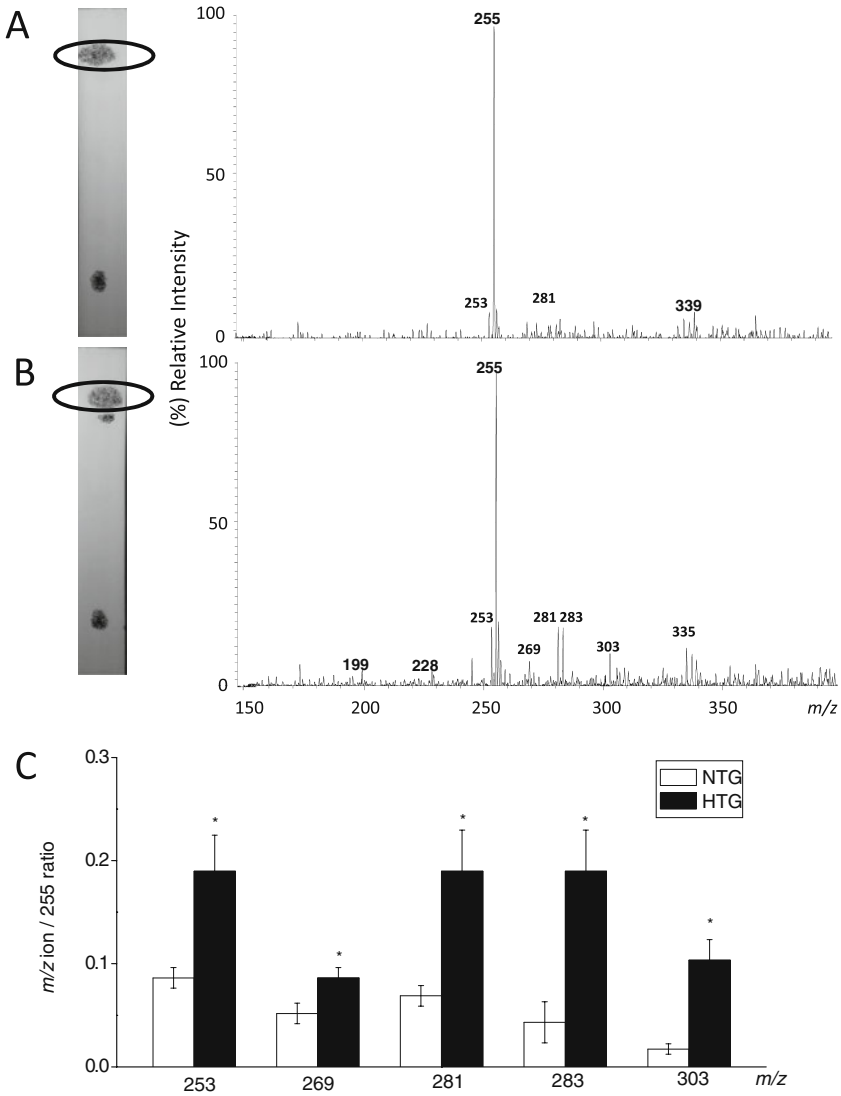

Fig. 3 On-spot HPTLC-EASI (−) mass spectra of three different liver extracts from **A** normotriglyceridemic and **B** hypertriglyceridemic mice. **C** Averages±SEM of ion intensities relative to *m/z* 780

total phospholipids. Differences in the nature and quantity of phosphatidylcholine can influence membrane fluidity, function, and interaction of phosphatidylcholine with enzymes that modulate lipid metabolism. The insertion of oleic acid into TAG and phosphatidylcholine could reflect the distinct FFA profile found in hypertriglyceridemic livers, which showed elevated relative abundances of oleic (18:1), palmitoleic (16:1), arachidonic (20:4), margaric (17:0), and stearic (18:0) acids. A higher relative abundance of phosphatidylinositol (38:4), the main phospholipid anchor of arachidonic acid in the cell membranes, was evidenced in hypertriglyceridemic livers. Therefore, as predicted by us, besides increased total TAG content [7], hypertriglyceridemic livers present a very distinct lipid profile compared with control normotriglyceridemic livers, independently of diet composition.

Margaric acid is a biological marker of diet fat composition [41], since it is not produced endogenously. It is synthesized by the bacterial flora in the rumen of ruminants [42] and incorporated into their tissues. Ruminants' tissues are used as raw material for rodent laboratory diets. Since both mice (hypertriglyceridemic and normotriglyceridemic) were subjected to the same diet, the increased relative abundance of the margaric acid reflects the higher food consumption of hypertriglyceridemic mice described by us previously [8]. Increase of oleic and palmitoleic acids has also been observed in earlier studies in livers from patients with diet-induced hypertriglyceridemia and in the plasma and livers of subjects with nonalcoholic fatty liver disease [43, 44].

The content of arachidonic acid containing phosphatidylinositol is an important source of cell signaling molecules such as the second messengers phosphatidylinositol–bisphosphate and phosphatidylinositol–triphosphate, and the arachidonic acid derived eicosanoids. Recently, ATP-sensitive potassium channel opening has been shown to respond to phosphatidylinositol-4,5-bisphosphate in isolated cardiac mitochondria [45], but its intracellular source is

unknown. In addition, products of arachidonic acid metabolism by CYP2J2 epoxygenase, epoxyeicosatrienoic acids, have been related to ATP-sensitive potassium channel activation after cellular stress in cardiomyocytes [46]. Thus, increased arachidonic acid-PI may be related to the described increased activity of ATP-sensitive potassium channel observed in hypertriglyceridemic mice [7, 9].

In conclusion, we showed that the EASI(±)-MS technique, one of the simplest ambient mass spectrometry techniques [21], is able to determine the phosphatidylcholine and TAG profiles of livers with no pre-separation steps and with very little sample preparation. To ascertain the FFA liver profile, however, pre-separation is required but a simple chromatographic separation by HPTLC is sufficient to enable EASI-MS on-spot detection. Using these techniques, representative lipid profiles of livers from genetic hypertriglyceridemic mice were obtained and compared with control normolipidemic mice. We demonstrated higher incorporation of oleic acid into phosphatidylcholine and TAG composition, higher content of phosphatidylinositol containing arachidonic acid, and overall distinct FFA profile in the livers of genetic hypertriglyceridemic mice. The features of the lipid profiles described here are certainly sufficient to change membrane physico-chemical proprieties and hence cell or organelles functions. In fact, liver mitochondria, spleen lymphocytes, and whole body metabolism are significantly increased in these hypertriglyceridemic mice. However, at this point, it is quite difficult to anticipate which particular alteration in lipid profile is cause or consequence of the alterations in the metabolic profile in this hyperlipidemic condition.

Acknowledgment This study is supported by grants from the Fundação de Amparo à Pesquisa do Estado de São Paulo (FAPESP) and Conselho Nacional de Desenvolvimento Científico e Tecnológico (CNPq).

References

1. Grundy SM, Brewer HB Jr, Cleeman JI, Smith SC Jr, Lenfant C (2004) Definition of metabolic syndrome: report of the National Heart, Lung, and Blood Institute/American Heart Association conference on scientific issues related to definition. Circulation 109:433–438
2. Marchesini G, Brizi M, Morselli-Labate AM, Bianchi G, Bugianesi E, McCullough AJ, Forlani G, Melchionda N (1999) Association of nonalcoholic fatty liver disease with insulin resistance. Am J Med 107:450–455
3. Reid AE (2001) Nonalcoholic steatohepatitis. Gastroenterology 121:710–723
4. Ito Y, Azrolan N, O'Connell A, Walsh A, Breslow JL (1990) Hypertriglyceridemia as a result of human apolipoprotein C-III gene expression in transgenic mice. Science 1249:790–793
5. Aalto-Setala K, Fisher EA, Chen X, Chajekshaul T, Hayek T, Zechner R et al (1992) Mechanism of hypertriglyceridemia in human apolipoprotein (apo) C-III transgenic mice: diminished very low density lipoprotein fractional catabolic rate associated with increased apoCIII and reduced apoE on the particles. J Clin Invest 90:1889–1900
6. De Silva HV, Lauer SJ, Wang J, Simonett WS, Weisgraber KH, Mahley RW et al (1994) Overexpression of human apolipoprotein C-III in transgenic mice results in accumulation of apolipoprotein B48 remnant that is corrected by excess apolipoprotein E. J Biol Chem 269:2324–2335
7. Alberici LC, Oliveira HC, Paim BA, Mantello CC, Augusto AC, Zecchin KG, Gurgueira SA, Kowaltowski AJ, Vercesi AE (2009) Mitochondrial ATP-sensitive K(+) channels as redox signals to liver mitochondria in response to hypertriglyceridemia. Free Radic Biol Med 47:1432–1439
8. Alberici LC, Oliveira HC, Bighetti EJ, de Faria EC, Degaspari GR, Souza CT, Vercesi AE (2003) Hypertriglyceridemia increases mitochondrial resting respiration and susceptibility to permeability transition. J Bioenerg Biomembr 35:451–457
9. Alberici LC, Oliveira HC, Patrício PR, Kowaltowski AJ, Vercesi AE (2006) Hyperlipidemic mice present enhanced catabolism and higher mitochondrial ATP-sensitive K + channel activity. Gastroenterology 131:1228–1234
10. Han X, Gross RW (2003) Global analyses of cellular lipidomes directly from crude extracts of biological samples by ESI mass spectrometry: a bridge to lipidomics. J Lipid Res 44:1071–1079
11. Han X, Gross RW (2005) Shotgun lipidomics: electrospray ionization mass spectrometric analysis and quantitation of cellular lipidomes directly from crude extracts of biological samples. Mass Spectrom Rev 24:367–412
12. Wenk MR (2005) The emerging field of lipidomics. Nat Rev Drug Discov 4:594–610
13. Christie WW (2009) Lipidomics—a personal view. Lipid Technology 21:58–60
14. Pulfer M, Murphy RC (2003) Electrospray mass spectrometry of phospholipids. Mass Spectrom Rev 22:332–364
15. Byrdwell WC (2001) Atmospheric pressure chemical ionization mass spectrometry for analysis of lipids. Lipids 36:327–346
16. Fuchs B, Schiller J (2009) Application of MALDI-TOF mass spectrometry in lipidomics. Eur J Lipid Sci Technol 111:83–98
17. Fuchs B, Schiller J, Süβ R, Zscharnack M, Bader A, Müller P, Schürenberg M, Becker M, Suckau D (2008) Analysis of stem cell lipids by offline HPTLC-MALDI-TOF MS. Anal Bional Chem 392:849–860
18. Touchstone JC (1995) Thin-layer chromatographic procedures for lipid separation. J Chromatogr B 671:169–195
19. Santos LS, Haddad R, Höehr NF, Pilli RA, Eberlin MN (2004) Fast screening of low molecular weight compounds by thin-layer chromatography and "on-spot" MALDI-TOF mass spectrometry. Anal Chem 76:2144–2147
20. Paglia G, Ifa DR, Wu C, Corso G, Cooks RG (2010) Desorption electrospray ionization mass spectrometry analysis of lipids after two-dimensional high-performance thin-layer chromatography partial separation. Anal Chem 82:1744–1750
21. Alberici RM, Simas CR, Sanvido GB, Romão W, Lalli PM, Benassi M, Cunha IBS, Eberlin MN (2010) Ambient mass spectrometry: bringing MS into the real world. Anal Bional Chem 398:265–294
22. Venter A, Neflieu M, Cooks RG (2008) Ambient desorption mass spectrometry. Trends Anal Chem 27:284–290
23. Harris GA, Nyadong L, Fernandez FM (2008) Recent developments in ambient ionization techniques for analytical mass spectrometry. Analyst 133:1297–1301
24. Van Berkel GJ, Pasilis SP, Ovchinnikova O (2008) Established and emerging atmospheric pressure surface sampling/ionization techniques for mass spectrometry. J Mass Spectrom 43:1161–1180

25. Haddad R, Sparrapan R, Eberlin MN (2006) Desorption sonic spray ionization for (high) voltage-free ambient mass spectrometry. Rapid Commun Mass Spectrom 20:2901–2905
26. Haddad R, Sparrapan R, Kotiaho T, Eberlin MN (2008) Easy ambient sonic-spray ionization-membrane interface mass spectrometry for direct analysis of solution constituents. Anal Chem 80:898–903
27. Haddad R, Milagres HMS, Catharino RR, Eberlin MN (2008) Easy ambient sonic-spray ionization mass spectrometry combined with thin-layer chromatography. Anal Chem 80:2744–2750
28. Eberlin LS, Abdelnur PV, Passero A, de Sá GF, Daroda RJ, Souza V, Eberlin MN (2009) Analysis of biodiesel and biodiesel–petrodiesel blends by high performance thin layer chromatography combined with easy ambient sonic-spray ionization mass spectrometry. Analyst 134:1652–1657
29. Walsh A, Azrolan N, Wang K, Marcigliano A, O'Connell A, Breslow JL (1993) Intestinal expression of the human apoA-I gene in transgenic mice is controlled by a DNA region 3′ to the gene in the promoter of the adjacent convergently transcribed apoC-III gene. J Lipid Res 34:617–623
30. Bligh EG, Dyer WJ (1959) A rapid method of total lipid extraction and purification. Can J Biochem Physiol 37:911–917
31. Yang L, Bennett R, Strum J, Ellsworth BB, Hamilton D, Tomlinson M, Wolf RW, Housley M, Roberts BA, Welsh J, Jackson BJ, Wood SG, Banka CL, Thulin CD, Linford MR (2009) Screening phosphatidylcholine biomarkers in mouse liver extracts from a hypercholesterolemia study using ESI-MS and chemometrics. Anal Bioanal Chem 393:643–654
32. Dill AL, Ifa DR, Manicke NE, Ouyang Z, Cooks RG (2009) Mass spectrometric imaging of lipids using desorption electrospray ionization. J Chromatogr B Analyt Technol Biomed Life Sci 877:2883–2889
33. Dill AL, Ifa DR, Manicke NE, Costa AB, Ramos-Vara JA, Knapp DW, Cooks RG (2009) Lipid profiles of canine invasive transitional cell carcinoma of the urinary bladder and adjacent normal tissue by desorption electrospray ionization imaging mass spectrometry. Anal Chem 81:8758–8764
34. Wiseman JM, Puolitaival SM, Takáts Z, Cooks RG, Caprioli RM (2005) Mass spectrometric profiling of intact biological tissue by using desorption electrospray ionization. Angew Chem Int Ed Engl 44:7094–7097
35. Nelson DL, Cox MM (2004) Lehninger principles of biochemistry. Freeman, New York
36. Manincke NE, Wiseman JM, Ifa DR, Cooks RG (2008) Desorption electrospray ionization (DESI) mass spectrometry and tandem mass spectrometry (MS/MS) of phospholipids and sphingolipids: ionization, adduct formation, and fragmentation. J Am Soc Mass Spectrom 19:531–543
37. Neelands PJ, Clandinin MT (1983) Diet fat influences liver plasma-membrane lipid composition and glucagon-stimulated adenylate cyclase activity. Biochem J 212:573–583
38. Simas RC, Catharino RR, Cunha IBS, Cabral EC, Barrera-Arellano D, Eberlin MN, Alberici RM (2010) Instantaneous characterization of vegetable oils via TAG and FFA profiles by easy ambient sonic-spray ionization mass spectrometry. Analyst 135:738–744
39. Picariello G, Sacchi R, Addeo F (2007) (2007) One-step characterization of triacylglycerols from animal fat by Maldi-Tof MS. Eur J Lipid Sci Technol 109:511–524
40. Perona JS, Barrón LJ, Ruiz-Gutiérrez V (1998) Determination of rat liver triglycerides by gas-liquid chromatography and reversed-phase high-performance liquid chromatography. J Chromatogr B Biomed Sci Appl 706:173–179
41. Wolk A, Furuheim M, Vessby B (2001) Fatty acid composition of adipose tissue and serum lipids are valid biological markers of dairy fat intake in men. J Nutr 131:828–833
42. Wu Z, Palmquist L (1991) Synthesis and biohydrogenation of FA by ruminal microorganisms in vitro. J Dairy Sci 74:3035–3036
43. Puri P, Wiest MM, Cheung O, Mirshahi F, Sargeant C, Min HK, Contos MJ, Sterling RK, Fuchs M, Zhou H, Watkins SM, Sanyal AJ (2009) The plasma lipidomic signature of nonalcoholic steatohepatitis. Hepatology 50:1827–1838
44. Puri P, Baillie RA, Wiest MM, Mirshahi F, Choudhury J, Cheung O, Sargeant C, Contos MJ, Sanyal AJ (2007) A lipidomic analysis of nonalcoholic fatty liver disease. Hepatology 46:1081–1090
45. Wojtovich AP, Williams DM, Karcz MK, Lopes CM, Gray DA, Nehrke KW, Brookes PS (2010) A novel mitochondrial K(ATP) channel assay. Circ Res 106:1190–1196
46. Katragadda D, Batchu SN, Cho WJ, Chaudhary KR, Falck JR, Seubert JM (2009) Epoxyeicosatrienoic acids limit damage to mitochondrial function following stress in cardiac cells. J Mol Cell Cardiol 46:867–875